Draft version December 11, 2023
Typeset using LaTeX **twocolumn** style in AASTeX631

Detailed analysis of photometry and spectroscopy of lensing clusters

Nikhil Garuda [1]

[1] *Department of Astronomy/Steward Observatory, University of Arizona, 933 N. Cherry Avenue, Tucson, AZ 85721, USA*

ABSTRACT

This study presents a detailed analysis of the lensing clusters particularly G165 at redshift z = 0.35, focusing on photometry and spectroscopy. Leveraging observations from JWST NIRCam/NIRSpec spectroscopy, the analysis explores the gravitational lensing effects, revealing the cluster's unique characteristics and providing insights into its mass estimation and luminosity. The photometry analysis, conducted using `SExtractor` and `EAZY` tools, emphasizes a nuanced understanding of multi-band photometry and photometric redshift estimation. Challenges in reconciling photometric and spectroscopic redshifts are discussed, attributing the ±0.2 dispersion to various observational factors. Detailed data processing methodologies, including PSF matching and image reprojection, are outlined, along with proposed enhancements to mitigate noise and improve uncertainties in flux measurements. The study highlights the limitations due to data availability and suggests strategies for future improvements in observational techniques. Overall, this analysis offers valuable insights into the complexities of lensing clusters, emphasizing the need for refined observational methodologies and data processing techniques to unravel the detailed composition and properties of such cosmic phenomena.

1. INTRODUCTION

It was long known since the early days of modern cosmology that the universe was expanding (Hubble (1929); Lemaître (1931); Hubble & Humason (1931)). During this time, Zwicky (1933) also suggested that there was some unseen matter that was the likely dominant mass component in clusters of galaxies. Zwicky (1937) further noted that gravitational lensing by clusters would be invaluable to: (i) trace and measure the amount of this unseen mass, now referred to as dark matter; and (ii) study magnified distant objects lying behind clusters.

Lensing clusters are very important part in the understanding of ΛCDM model of our universe and gives us an insight of how it was created.

2. MOTIVATION

For the purposes of this project, we will be understanding the photometry of the clusters that can be further be used in lens models to make detailed analysis on the amount of baryonic and dark matter in the cluster. We will be then also testing the reliability of the photometry using the spectroscopy either extracted from the datasets mention in §3.1 or using archival data from `MAST`.

Due to time constraints, we were only able to focus on one cluster, namely, PLCK G165.7+67.0 (hereafter G165), which shows strong-lensing constraints in the form of giant arcs and image multiplicities.

2.1. *G165*

The galaxy cluster G165 ($z = 0.35$) first got attention by gravitationally amplifying a single, apparently-bright galaxy in the background. It was boosted to an observed sub-mm flux density of $S_{350\mu m} > 700$ mJy (Cañameras et al. (2015); Harrington et al. (2016)), making it detectable by the *Planck* and *Herschel Space Observatory* missions (Ade et al. (2016); Aghanim et al. (2020)).

G165 is a double-cluster with two prominent cluster cores, its X-ray luminosity is lower than galaxy clusters of a similar redshift, and its mass, based on the *Planck* SZ Compton-Y map, yields only an upper limit. These properties arise in part because the cluster has a relatively-small mass of $2 - 3 \times 10^{14} M_{\odot}$ (Frye et al. (2019); Pascale et al. (2022)), and in part because the source responsible for the high restframe far-infrared flux density is not the entire galaxy cluster but a only portion of a single lensed source that is a dusty and high star forming galaxy (DSFG).

nikhilgaruda@arizona.edu

HST WFC3-IR imaging enabled the identification of large sets of image systems and the construction of lens models (Frye et al. (2019)). These models confirmed both the northeastern (NE) and southwestern (SW) cores of this binary cluster, and the high, cluster-scale mass. This earlier work was built and expanded upon by the addition of robust photometric redshift estimates across ground and space-based data sets for three of the 11 image systems and several cluster members (Pascale et al. (2022)). Yet, these models were anchored on the spectroscopic redshift for only one image system, thereby limiting the accuracy of the resulting lens model and its ability to recover the lensed image positions (Johnson & Sharon (2016)).

Additional, observations were taken using JWST/NIRCam as a part of the Prime Extragalactic Areas for Reionization and Lensing Science (PEARLS) program (Windhorst et al. (2022)) and also as part of a JWST disruptive DDT program (PID 4446, PI: Frye) that had a detailed analysis covered in Frye et al. (2023).

3. DATA

3.1. *Datasets*

The observations for this project were done using NIRCam that was obtained as part of a JWST disruptive DDT program (PID 4446, PI: Frye) to follow the supernova's light curve in each of its three images. Exposures were taken in six filters using only Module B of NIRCam. The exposure times are recorded in Table 1. We will only be using one of the epochs for this project (Epoch 3).

Filter	Exposure
F090W	1417
F115W	...
F150W	1246
F200W	1761
F277W	1761
F356W	1246
F410M	...
F444W	1417

Table 1. JWST Filters and NIRCam Exposure Times in seconds for Epoch 3.

NIRSpec medium-resolution Micro-Shutter Array (MSA) spectroscopy of the G165 field was obtained on 2023 Apr 22. The MSA mask was populated with the positions of the three SN appearances and two of the three images of the SN host galaxy, followed by counter-images of three other image systems. The remainder of the mask was filled with other lensed sources which summed to a total of 42 lensed targets.

The observations used the grating/filter combinations G140M/F100LP to cover spectral range 0.97–1.84 μm (rest-frame 0.35–0.66 μm at $z = 1.8$) and G235M/F170LP to cover 1.66–3.17 μm ($z = 1.8$ rest-frame 0.57–1.1 μm), both with spectral resolution R $\sim$ 1000. There was also a PRISM/CLEAR spectrum covering 0.7–5.3 μm (rest-frame 0.25–1.9 μm) with R $\sim$ 20–300 (50–14 $\AA$).

3.2. *Data Processing*

This report only covers the processing of the images for the photometry and there will be a separate report (Matlock in prep.) that will focus on the spectroscopy aspect of this project.

We first obtained the images via `MAST` and the latest photometric calibration files were used (pmap_1126). All the Short Wavelength (SW) and Long Wavelength (LW) images were then isolated to obtain the science and weight images.

We then reprojected all the SW and LW images to a constant pixel scale of 0.06" as that is the scale of the detection image (F444W). This was doing using Astropy packages `reproject` and `astroalign`. `Astroalign` outperforms `reproject` in producing astrometrically precise image alignment, but fails when images are significantly misaligned. Hence, we first apply `reproject`, which transforms images to the same orientation and pixel scale based on the World Coordinate System (WCS) header information. We then follow up on this step by applying the `astroalign` task in order to triangulate the source centroid positions and to calculate a revised value for the reprojection according to Beroiz et al. (2020).

3.3. *PSF Matching*

Using the matched images, each image was convolved with a kernel to match the PSF of the F444W image. Each kernel was created using `webbpsf` with an oversampling value. Then we create a matching kernel by taking the ratio of the PSF of the two images as per convolution theorem. This therefore is the integral of two quantities is equivalent to their multiplication in Fourier space. By convolution theorem, $K = \mathcal{F}^{-1}(\mathcal{F}(\mathrm{PSF}_1/\mathcal{F}(\mathrm{PSF}_2))$. We also apply a simple Cosine window function prior to convolution to eliminate any spurious modes picked up by noise. This procedure is adapted from (Pascale et al. (2022)).

4. PHOTOMETRY

4.1. *SExtractor*

We perform multi-band photometry using `SExtractor` (Bertin & Arnouts (1996)) by implementing a two-step *HOT+COLD* method according to prescription in Galametz et al. (2013). The *COLD* parameter is tuned to detect bright, extended galaxies while the *HOT* parameter is set to be optimized to detect fainter galaxies not included in the preceeding *COLD* mode run. The `SExtractor` used to make the initial object catalog is described in Table 2.

The JWST NIRCam F444W image was assigned as the reference image since it corresponds to the diffraction limit of the telescope. All the images are matched to this reference image with the procedure aforementioned in §3.3. This lets us disregard aperture corrections and use the approaches of Merlin et al. (2022); Paris et al. (2023) to make the final multi-band photometry catalog. These procedures balance the need to make faint image detections while also limiting the introduction of spurious sources.

Parameter	Value
DETECT_MINAREA	10
DETECT_THRESH	2.0
ANALYSIS_THRESH	2.5
DEBLEND_NTHRESH	64
DEBLEND_MINCONT	0.0001

Table 2. SExtractor Parameters for the object catalogs

The final photometry catalog utilises the procedures mentioned above using circular apertures for each source of diameter 0".66 . This was done since the study for this project doesn't have a key focus on the extended galaxies but rather general understanding of detailed photometry analysis for lensing clusters.

4.2. *EAZY*

For the purposes of this project, we used EAZY (Brammer et al. (2008)) to estimate photometric redshifts. SED templates were optimised for identification of galaxies using FSPS templates.

We were able to match only 7 sources with the spectroscopy sources that were in Frye et al. (2023). Overall, there has been a dispersion of ± 0.2 in z which was to be expected due to pitfalls of having lower exposure times in the Epoch 3 and also different pixel scales in SW and LW filters.

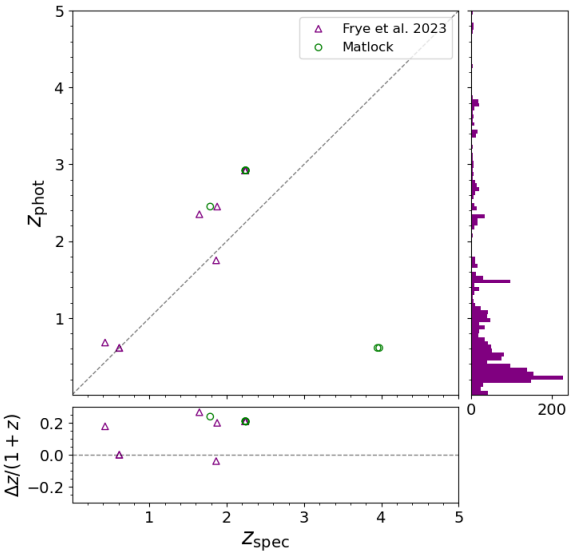

Figure 1. Photometric vs. spectroscopic redshifts. Points depict redshifts by (Matlock in prep; Frye et al. (2023)) as indicated in the legend. The panel on the right gives the histogram of photometric redshifts using EAZY.

A photometric redshift is considered secure if the object is: (1) in the field-of-view for all filters, (2) detected in a minimum of six filters, and (3) spatially resolved from its neighbors. The pitfalls of the photometric redshifts will be further discussed in §5.

Here is a Spectral Energy Distribution (SED) plot for one the sources that has very similar photometric and spectroscopic redshift.

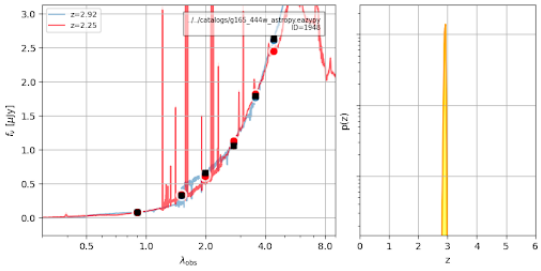

Figure 2. SED of source NS 46 from Frye et al. (2023). The blue SED is the model templates for the redshift obtained from EAZY and the red is the model from the spectroscopic redshift from (Matlock in prep.).

5. DISCUSSIONS

In order to check the reliability of the catalog we made some color-color and color-magnitude plots to test if the catalog was similar to (Frye et al. (2023)).

As mentioned in §3, we only were able to analyse one of the three epochs (Epoch 1 is proprietary). Due to this, we weren't able to get the full coverage and were not

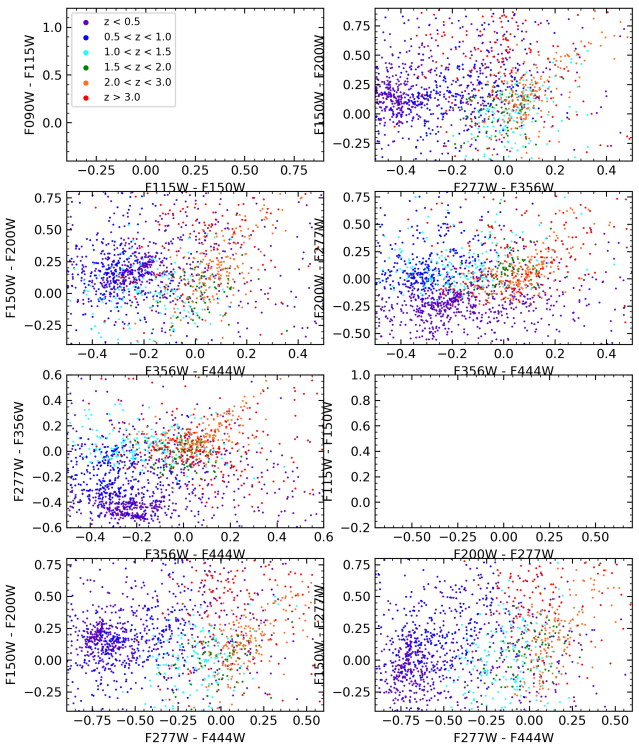

Figure 3. Color vs Color plot made for this project using Epoch 3. Only 6 out of 8 filters are available for this epoch and the the colors are a function of increasing redshift.

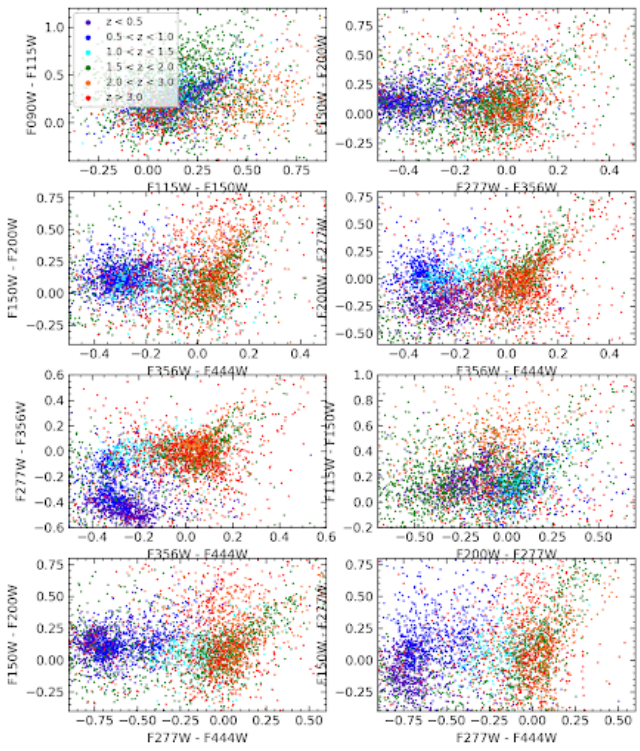

Figure 5. Color vs Color plot made with the catalog obtained from the original paper (Pascale priv. comm.). The colors are a function of increasing redshift.

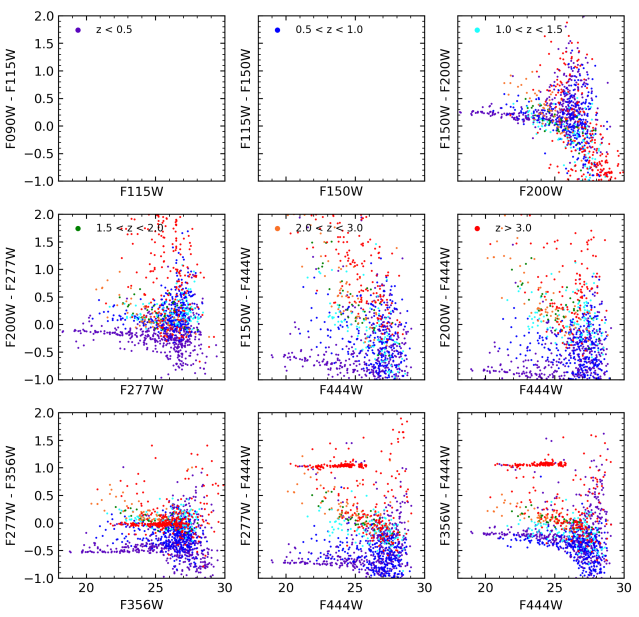

Figure 4. Color vs Magnitude plot made for this project using Epoch 3. Only 6 out of 8 filters are available for this epoch and the colors are a function of increasing redshift.

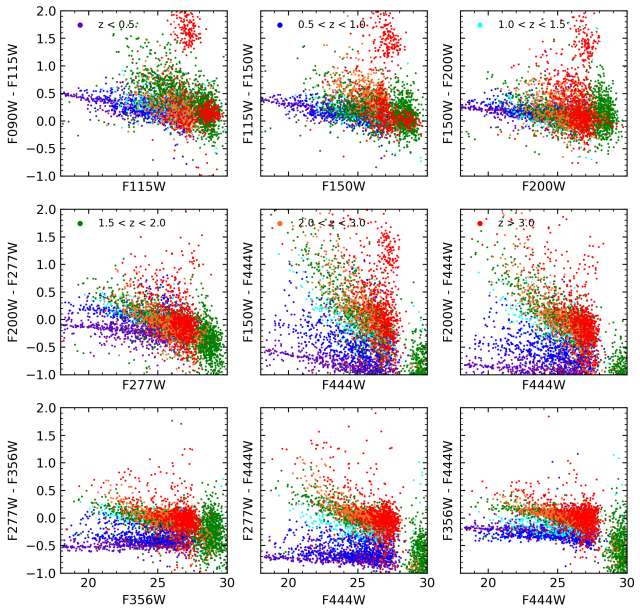

Figure 6. Color vs Color plot made with the catalog obtained from the original paper (Pascale priv. comm.). The colors are a function of increasing redshift.

able to get a lot more exposure time as well. Some of the things we could improve upon with the image processing

steps would be to do an additional correction for the $1/f$ noise by applying the prescription of C. Willott[1].

We can also do additional correction for detector-level offsets, "wisps," and "snowballs" (Robotham et al. (2018, 2023, 2017))though it is out of scope for the purposes of this project. One thing that can surely improve the image qualities would be to create a combined mosaic using the process was similar to that first described by Koekemoer et al. (2011). This process combines all the epochs and also does the pixel scale correction that will improve the PSFs and the photometry by a lot.

On the photometry side, we can improve the uncertainties of the fluxes obtained by injecting 5000 point sources from `WebbPSF` of known fluxes into blank regions of the images, and fluxes and uncertainties were estimated using 0."1 apertures using `photutils` with the RMS maps associated with the images. This will give more realistic uncertainties similar to Frye et al. (2023).

Another place of improvement, would be to also do correction for extended sources using isophotal photometry and making a separate catalog for that. One thing we could also do is to use templates that is curated for JWST/NIRCam like that of Larson et al. (2023).

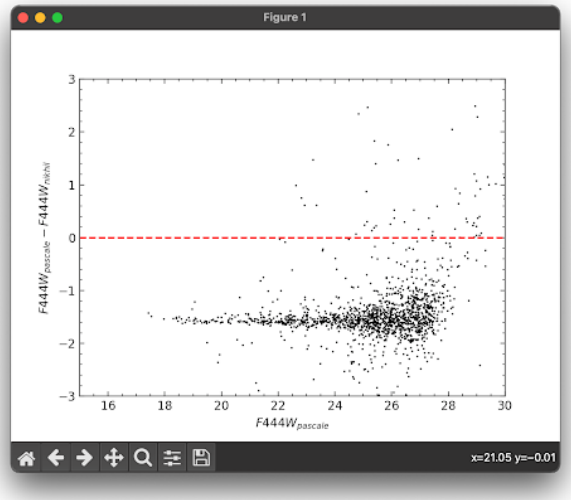

Figure 7. Difference in magnitudes with both the catalogs to show the shift in magnitudes. Acts as a source of improvement.

6. CONCLUSIONS

The analysis of G165's lensing effects and photometric-spectroscopic interplay offers valuable insights into understanding the cluster's composition, limitations in measurements, and avenues for refining observational methodologies. Continued improvements in data processing and analysis techniques promise advancements in unraveling the mysteries of lensing clusters.

REFERENCES

Ade, P., Aghanim, N., Argüeso, F., et al. 2016, Astronomy & Astrophysics/Astronomie et Astrophysique, 594

Aghanim, N., Akrami, Y., Ashdown, M., et al. 2020, Astronomy & Astrophysics, 641, A6

Beroiz, M., Cabral, J. B., & Sanchez, B. 2020, Astronomy and Computing, 32, 100384, doi: 10.1016/j.ascom.2020.100384

Bertin, E., & Arnouts, S. 1996, A&AS, 117, 393, doi: 10.1051/aas:1996164

Brammer, G. B., van Dokkum, P. G., & Coppi, P. 2008, The Astrophysical Journal, 686, 1503

Cañameras, R., Nesvadba, N., Guery, D. e. a., et al. 2015, Astronomy & Astrophysics, 581, A105

Frye, B. L., Pascale, M., Qin, Y., et al. 2019, The Astrophysical Journal, 871, 51

Frye, B. L., Pascale, M., Pierel, J., et al. 2023, arXiv preprint arXiv:2309.07326

Galametz, A., Grazian, A., Fontana, A., et al. 2013, The Astrophysical Journal Supplement Series, 206, 10

Harrington, K., Yun, M. S., Cybulski, R., et al. 2016, Monthly Notices of the Royal Astronomical Society, 458, 4383

Hubble, E. 1929, Proceedings of the National Academy of Science, 15, 168, doi: 10.1073/pnas.15.3.168

Hubble, E., & Humason, M. L. 1931, Astrophysical Journal, vol. 74, p. 43, 74, 43

Johnson, T. L., & Sharon, K. 2016, The Astrophysical Journal, 832, 82

Koekemoer, A. M., Faber, S., Ferguson, H. C., et al. 2011, The Astrophysical Journal Supplement Series, 197, 36

[1] https://github.com/chriswillott/jwst.git

Larson, R. L., Hutchison, T. A., Bagley, M., et al. 2023, The Astrophysical Journal, 958, 141

Lemaître, G. 1931, MNRAS, 91, 483, doi: 10.1093/mnras/91.5.483

Merlin, E., Bonchi, A., Paris, D., et al. 2022, The Astrophysical Journal Letters, 938, L14

Paris, D., Merlin, E., Fontana, A., et al. 2023, arXiv preprint arXiv:2301.02179

Pascale, M., Frye, B. L., Dai, L., et al. 2022, The Astrophysical Journal, 932, 85

Robotham, A., Davies, L., Driver, S., et al. 2018, Monthly Notices of the Royal Astronomical Society, 476, 3137

Robotham, A., D'Silva, J., Windhorst, R., et al. 2023, Publications of the Astronomical Society of the Pacific, 135, 085003

Robotham, A., Taranu, D., Tobar, R., Moffett, A., & Driver, S. 2017, Monthly Notices of the Royal Astronomical Society, 466, 1513

Windhorst, R. A., Cohen, S. H., Jansen, R. A., et al. 2022, The Astronomical Journal, 165, 13

Zwicky, F. 1933, Helvetica Physica Acta, Vol. 6, p. 110-127, 6, 110

—. 1937, Physical Review, 51, 290